Kinematic of focusing regions

2014 J. Opt. 16 085704

(http://iopscience.iop.org/2040-8986/16/8/085704)

IOP Publishing Journal of Optics
J. Opt. 16 (2014) 085704 (7pp) doi:10.1088/2040-8978/16/8/085704

Kinematic of focusing regions

G Martínez-Niconoff[1], S I De los Santos G[1], J Silva-Barranco[1], J A Martínez-Martínez[1], P Martínez-Vara[2] and J C Ramírez-San-Juan[1]

[1] Instituto Nacional de Astrofísica Óptica y Electrónica INAOE, Dpto. de Óptica, Postal 51 y 216, Puebla, México
[2] Benemérita Universidad Autónoma de Puebla, BUAP Dpto. de Ingeniería, México

E-mail: gmartin@inaoep.mx

Received 14 March 2014, revised 3 June 2014
Accepted for publication 9 June 2014
Published 25 July 2014

Abstract

We describe the interaction between focusing regions and analyze the resulting physical features. The study is supported by the fact that focusing regions exhibit particle-like behavior and the interaction among these presents features similar to inelastic collision. When focusing regions are generated in a medium with random refractive index, the irradiance distribution along the focusing regions changes according to the diffusion process and the collision between them generates vortex-like effects. This study was implemented by solving the irradiance transport equation. Experimental results are in good agreement with the theoretical model performed.

Keywords: focusing regions, diffusion process, irradiance transport equation

(Some figures may appear in colour only in the online journal)

1. Introduction

The physical properties of an optical field can be obtained from the wavefront, which is a surface that can be represented in parametric form as [1, 2]

$$x(u, v), \quad y = y(u, v), \quad z = z(u, v). \tag{1}$$

In order to obtain the mathematical representation of the wavefront geometry $z = F(x,y)$, free of the parameters (u,v), the parametric functions (1) must be invertible and the determinant of the transformation matrix must be different to zero:

$$\det M(u, v) = \det\begin{pmatrix} x_u & x_v \\ y_u & y_v \end{pmatrix} \neq 0, \tag{2}$$

where $(x_{u,v}, y_{u,v})$ represents the partial derivatives. Then we have that the transformation matrix has rank 2; however, optical regions exist where the matrix rank is smaller than 2, which is the mathematical definition of singularity. In the neighborhood of these singular regions, interesting physical features appear, which are analyzed in the present manuscript. When the matrix rank is 0, the singularity corresponds to a point, and when the matrix rank is 1 it is a curve [1]. From these results, we know that the geometry of optical singularities is either points or curves. Singularities are also known as focusing regions or caustics and these are generated by the envelope of a set of trajectories orthogonal to the wavefront [3–7].

In the present manuscript, we focus on investigating the interaction between two focusing regions, which implies dynamic focusing regions. These can be generated in a medium with random refractive index whose statistical parameters are time-dependent. To maintain a geometrical point of view, we propose that the random fluctuations of the refractive index are equivalent to a dynamic rough surface in the sense that both of them generate the same focusing regions. We will show that such interaction produces irradiance redistribution, generating light that is guided along the focusing regions. During the interaction period, part of the energy modifies the geometry of the focusing region while another may generate vortex-like effects, both these features being analyzed in the present study. The analysis is supported by the fact that focusing regions exhibit adiabatic features [8, 9], which means that such optical fields have particle-like features and the interaction between focusing regions can be modeled as a kind of collision between particles, establishing a direct analogy with mechanical systems.

The spatio-temporal evolution of focusing regions presents two important features, the first of which is the behavior of focusing regions free of interaction. Its evolution in a medium with random refractive index generates morphologic changes following a diffusion process. Another important

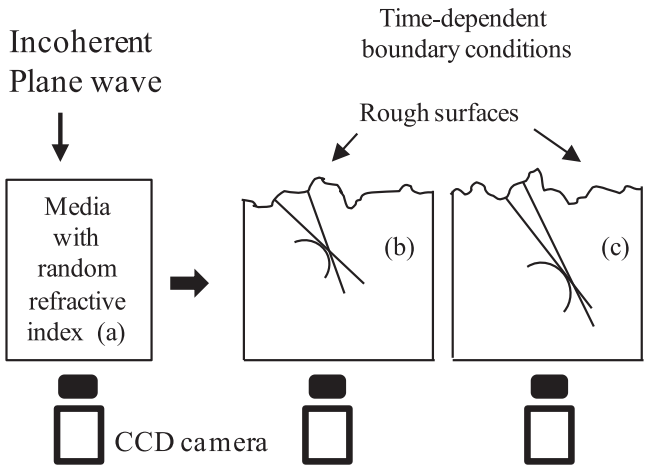

Figure 1. (a) Experimental set-up to generate the interaction between focusing regions. (b) and (c) show the equivalent systems for two times. In (a), the focusing region is generated by the propagation of a plane wave through a random medium. In (b) and (c), the focusing region is generated by orthogonal trajectories to the rough surface for two different times.

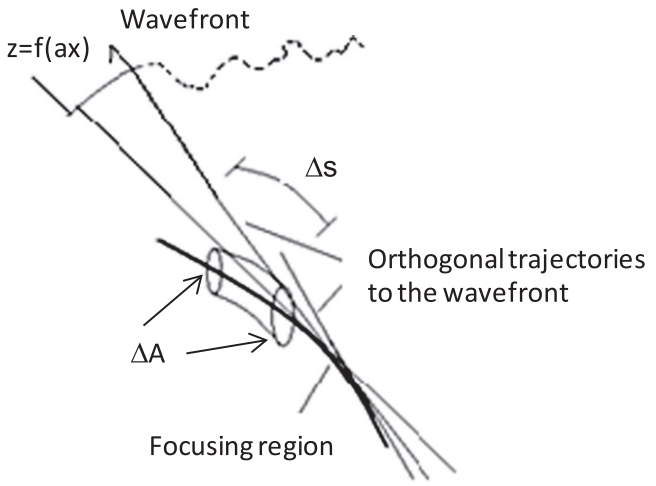

Figure 2. Synthesis of the focusing region using the envelope of a ray set.

feature occurs during the interaction between two focusing regions whose behavior is similar to an inelastic collision, which means that focusing regions are linked to each other at the contact point. This interaction is analyzed from the irradiance transport equation [10–12] and is implemented experimentally by propagating a plane wave through a medium with random refractive index. The medium is obtained by heating water up to ~80 °C and allowing it to cool down until it reaches room temperature. The refractive index may takes values in the interval of $n(20\,°C)$– $n(80\,°C)$. The water's temperature is non-uniform generating the random refractive index. Illuminating the water container with a plane wave, the optical field generates dynamic focusing regions whose interaction is detected with a CCD camera.

2. Description and synthesis of focusing regions

To describe the physical features of focusing regions and to pave the way, we maintain a geometric point of view. The type of fluctuation of the refractive index in regard to volume is equivalent to a random boundary condition which is interpreted as a rough surface whose profile changes with time, as seen in figure 1. This fact is justified in the appendix A. In this way, the two systems are equivalent in the sense that both generate the same focusing regions. As a consequence of the central limit theorem, we assume that the height distribution for the equivalent rough surface follows a Gaussian probability density function with time-dependent variance [13–14], represented by

$$\rho(z,\,t) = \frac{1}{\sqrt{2\pi}\,\sigma(t)}\exp\left(-\frac{z^2}{2\sigma(t)}\right). \tag{3}$$

It is well known that this function satisfies the diffusion equation. This property allows one to maintain a geometric point of view, which is necessary to explain the kinematic of focusing regions. In figure 1 we try to sketch the fact that only some regions of the rough surface generate a focusing region whose local profile is given by $z=f(ax)$, where $a(t)$ changes as a function of time. Some other interesting properties of focusing regions can be founded in [15]. Therefore, we can select a set of orthogonal trajectories to the boundary condition, generating an envelope curve that is the focusing region under study.

The focusing region corresponds to the envelope of the curvature centers of the boundary condition $y=f(ax)$, and the mathematical expression for the curvature center $(\alpha,\,\beta)$ is given by [1, 2, 9]:

$$\alpha(x,\,a) = x - \frac{y'\left(1+a^2y'^2\right)}{ay''},$$
$$\beta(x,\,a) = y + \frac{\left(1+a^2y'^2\right)}{ay''}. \tag{4}$$

From these expressions, it is easy to identify the nonlinear behavior of the focusing region, characterized by the change in arc length s, whose mathematical expression is given by

$$\Delta s = \int_1^{a_f}\frac{1}{y''}\sqrt{y'^2\left(\tfrac{1}{a^2}-y'^2\right)^2+\frac{4}{a^6y''^2}}\,\mathrm{d}a, \tag{5}$$

where it will be noted that minor changes in the parameter a imply major changes in the geometry of the focusing region. As a consequence, the irradiance is continuously redistributed along the focusing region. Previous statements can be resumed in figure 2, which shows the synthesis of an envelope curve, where a high density of trajectories is identified in the neighborhood of the focusing regions and thus optical diffusion processes are expected.

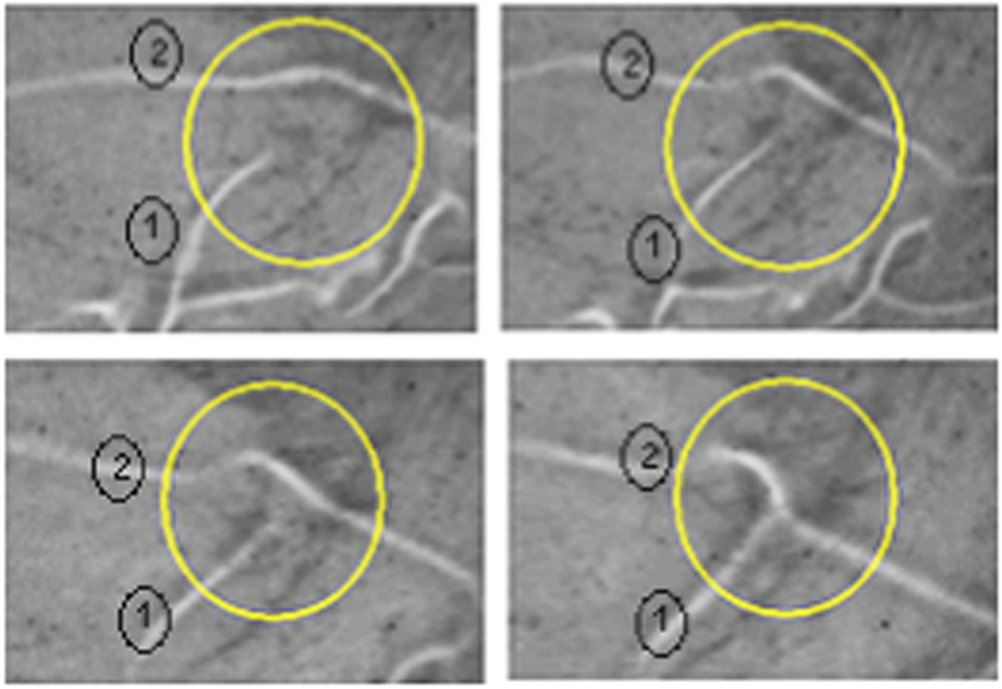

Figure 3. The circles enclose the diffusion process for the focusing region (1), which moves toward the focusing region (2) until they are linked at the contact point. The duration of the process was ∼1 s, using sunlight as light source.

3. Diffusion process on the focusing regions

In the appendix B, we show in a rigorous way that the irradiance function satisfies the diffusion differential equation,

$$\frac{\partial^2 I}{\partial s^2} = D\frac{\partial I}{\partial t}, \tag{6}$$

where s is the arc length, I is the irradiance function, and D is the diffusion constant. Note that the type of random fluctuation of the refractive index has a Gaussian probability density function, which is a consequence of the central limit theorem. Given that the trajectories that generate the focusing region are orthogonal to the wavefront, it is expected that the diffusion effects will appear along the focusing region, which necessary is a curve according with the definition of singularity.

The diffusion equation supports solutions with time decreasing exponential dependence, and the entire solution is given by

$$I(x, y, z, s, t) = I_0(x, y, z)\cos(\beta s + \mu)\exp(-ht), \tag{7}$$

where μ is a phase constant, the harmonic term describes light guided along the arc length. The structure of the boundary condition for the diffusion equation given by $I_0(x,y,z)$, must satisfy the irradiance transport equation [11] and this will be analyzed in the following section.

To corroborate the diffusion process, we propagate a plane wave thought a media with random refractive index generated by heating water. The experimental results obtained are shown in the sequence of images in figure 3. The region of interest is enclosed in a circle of approximately 5 mm of diameter, in fact the focusing regions are easily detected even without an additional optical system. The focusing regions are denoted by (1) and (2) and were detected using a CCD camera as is shown in figure 1. The end point of region (1) moves toward the focusing region (2) until it reaches it and is then linked at the contact point, analogous to an inelastic collision. This last behavior will be explained below. As an interim conclusion, the irradiance for a focusing region in a random medium changes its geometry following a diffusion process manifested along the arc length.

4. Interaction between focusing regions

The next focus of the study is to analyze the interaction between two focusing regions. We assume that a plane wave is propagated along the z-coordinate and that the changes in irradiance are detected on the transversal plane, x–y. The spatial part of the irradiance function represented by $I_0(x,y,z)$ satisfies the irradiance transport equation, given by

$$\nabla_\perp \cdot \left(I_0(x, y, z)\,\nabla_\perp L(x, y, z)\right) = \frac{\partial}{\partial z} I_0(x, y, z), \tag{8}$$

where L is the phase function and $\nabla_\perp$ is the transversal Laplace operator. Because the refractive index changes randomly, the morphology of the focusing region also changes. A geometrical idea of the interaction between focusing regions is shown in figure 4.

To describe the physical features of the interaction, we propose that at the contact point (x,y,z) the irradiance is given

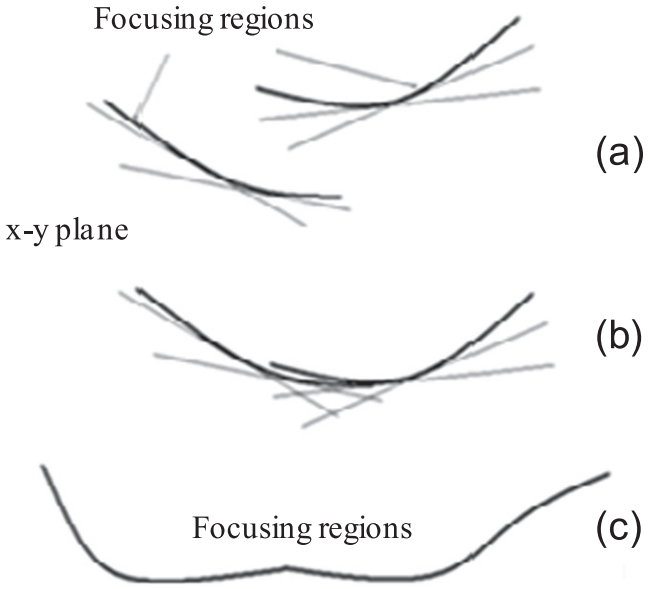

Figure 4. In (a), focusing regions are generated by the envelope of trajectories; (b) interaction between two focusing regions; (c) new focusing region.

by

$$I(x, y, z) = I_1(x, y, z) + I_2(x, y, z), \tag{9}$$

and the phase function is given by a phase difference between the corresponding optical fields, i.e.

$$L(x, y, z) = L_1(x, y, z) - L_2(x, y, z). \tag{10}$$

Substituting (9) and (10) in the irradiance transport equation, we obtain

$$\begin{aligned} &\nabla_\perp I_1 \cdot \nabla_\perp L_1 + I_1 \cdot \nabla_\perp^2 L_1 \\ &-\nabla_\perp I_2 \cdot \nabla_\perp L_2 - I_2 \cdot \nabla_\perp^2 L_2 \\ &+ \nabla \cdot \left(I_1 \nabla_\perp L_2 - I_2 \nabla_\perp L_1\right) \\ &= -\frac{\partial I_1}{\partial z} - \frac{\partial I_2}{\partial z}, \end{aligned} \tag{11}$$

where the interaction between the focusing regions is determined by the term $I_{\text{int}} = \nabla \cdot \left(I_1 \nabla_\perp L_2 - I_2 \nabla_\perp L_1\right)$. We define the irradiance density current as the vector function

$$J_{12} = I_1 \nabla_\perp L_2 - I_2 \nabla_\perp L_1. \tag{12}$$

During the period of interaction the irradiance is flowing along the focusing region, which must satisfy the continuity equation as a consequence of energy conservation:

$$\nabla \cdot J_{12} = \frac{\partial I_{12}}{\partial t}, \tag{13}$$

where I_{12} is the irradiance flowing between the focusing regions. An unexpected result was identified in the sequence of images shown in figure 5. At the contact point the focusing regions are linked and demonstrate a tendency to generate a single focusing region. During the period of interaction one of the focusing regions became brighter, which is experimental evidence of the irradiance flowing along the focusing region. When the interaction stopped, the irradiance density current $\boldsymbol{J_{12}}$ becomes zero:

$$I_1 \nabla_\perp L_2 - I_2 \nabla_\perp L_1 = 0, \tag{14}$$

and the gradient vectors are parallel:

$$\nabla_\perp L_2 = \frac{I_2}{I_1} \nabla_\perp L_1. \tag{15}$$

The physical interpretation of equation (15) is that the irradiance interaction has the structure of an inelastic collision, meaning that the two focusing regions are joined generating a single focusing region as it is shown by the sequence of images in figure 5. It should be noted that the focusing regions are linked at the contact point and a tendency to increase the number of contact points is observed, thereby generating a single focusing region.

Another important feature is the generation of vortex-like features whose structure can be obtained taking the curl of equation (12), obtaining

$$\nabla_\perp \times J = \nabla_\perp I_1 \times \nabla_\perp L_2 - \nabla_\perp I_2 \times \nabla_\perp L_1. \tag{16}$$

The modulus of the curl depends mainly on the sign of each term, which is related to the curvature of the focusing regions. When the curvature vector of each focusing region has the same sign, the curl modulus has a low value and the kinematic of the linked focusing regions is mainly translation. When the curvature vector has an opposite sign, the curl takes higher values and it has vortex-like behavior. These two scenarios are illustrated in figure 6, and the experimental results shown in figure 7 reinforce the previous comments, where vortex-like features are evident.

5. Conclusions

In conclusion, we analyzed the kinematic of focusing regions, to perform this study was necessary to generate dynamic focusing regions, it was possible by propagating light trough a media with random refractive index. We can distinguish two important features: (1) we demonstrate that the morphological changes of a single focal region follows a diffusion process, due to the singularities has curve shape, the diffusion process is manifested by changes in the arc length and curvature of the focusing region. (2) Another unexpected feature is that the interaction between focusing regions shows a similarity to inelastic collisions, it occurs when the focusing regions collide and then are linked at the contact point. To describe this interaction we used the irradiance transport equation which allows identifying the term that describes how the irradiance and phase of each focusing regions is redistributed. From this term, vortex-like features can be observed, establishing a similarity to mechanical systems because the vortex structure is related to the transport of angular momentum.

The experimental results are in good agreement with the theoretical model performed. Finally, as a consequence of the mechanical analogy, focusing regions can be described by means of their center of irradiance, which is analogous to the center of mass. The presented study can be used for dynamic optical trapping and the development of optical motors. The

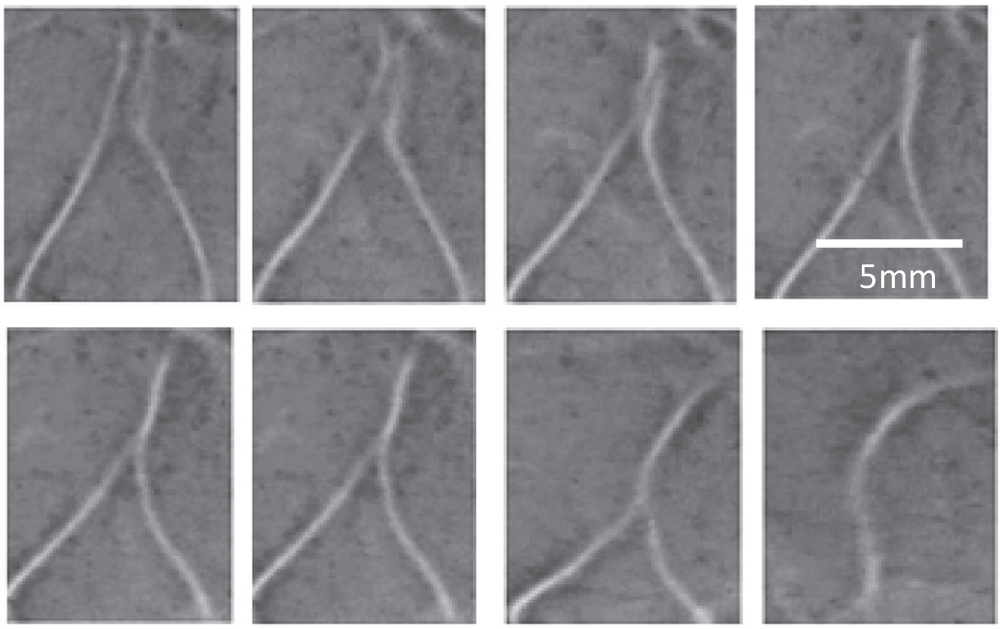

Figure 5. Experimental interaction between two focusing regions. The interaction has similar features to an inelastic collision. The time duration of the process was ∼1 s.

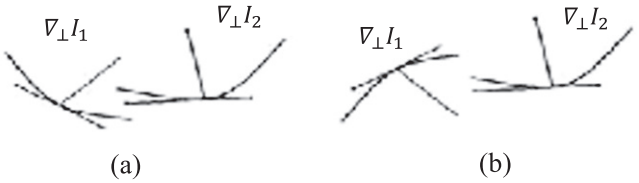

Figure 6. The interaction between two focusing regions depends on the curvature sign. In (a) both focusing regions have the same curvature sign while in (b) they have opposite signs.

foregoing comments will be explained using our model and presented in a forthcoming paper.

Appendix A. Equivalence between the volume media with random refractive index with the dynamic rough surface

In this appendix we show the equivalence between the light propagation trough a media with random refractive index and the diffraction field emerging from a rough surface. The study is performed by interpreting the random media as an array of thin slices depending on x–y spatial coordinates and time as it is sketched in figure A.1. Therefore, each slide can be interpreted as a random phase transmittance, the representation for the ith transmittance is given by $T_i(x,y,t)$. Then, the light propagation trough the volume of the random media is equivalent to analyze the light propagation through a set of transmittances in a tandem array.

The transmittance set is illuminated by a point source placed a distance z from the surface as it is sketched in figure A.1.

By considering a single one transmittance, the diffraction field in the Fraunhofer region, corresponds to the Fourier transform of the transmittance function given by

$$\begin{aligned}&\varphi(u, v, z=0)\\&=\int_{-\infty}^{\infty}\int_{-\infty}^{\infty} t_1(x, y)\exp\left(-i2\pi\left(xu+yv\right)\right)\mathrm{d}x\mathrm{d}y\\&=T_1(u, v),\end{aligned}\tag{A.1}$$

where $u = x_0/\lambda z$, $v = y_0/\lambda z_1$, and z_1 is the distance from the light source to the transmittance plane. We remark that the distance z_1 appears as a scale factor in the Fourier transform, and it can be proof that it is synthesized, in a virtual way, on the source plane.

Considering now, the propagation trough the second transmittance, the Fraunhofer diffraction field acquires the form of the convolution function between the Fourier transforms of each transmittance given by:

$$\begin{aligned}&\varphi(u, v, z=0)\\&=\int_{-\infty}^{\infty}\int_{-\infty}^{\infty} t_1(x, y, t)\, t_2(x, y, t)\\&\quad\times\exp\left(-i2\pi\left(xu+yv\right)\right)\mathrm{d}x\mathrm{d}y\\&=T_1(u, v, t)\otimes T_2(u, v, t),\end{aligned}\tag{A.2}$$

where $\otimes$ represents the convolution. Taking into account the complete set of transmittances, the Fraunhofer diffraction field takes the form:

$$\begin{aligned}&\varphi(u, v, z=0, t)\\&=\int_{-\infty}^{\infty}\int_{-\infty}^{\infty} \Pi\bar{T}_i(x, y, t)\exp\left(-i2\pi\left(xu+yv\right)\right)\mathrm{d}x\mathrm{d}y\\&=T_1(u, v)\otimes T_2(u, v)\ldots\otimes T_n(u, v)\\&=T(u, v, t).\end{aligned}\tag{A.3}$$

This equation implies that the Fraunhofer diffraction field associated to the set of transmittances in a tandem array is generated, in a virtual way, on the source plane. It is easily corroborated by watching the light source trough the random media.

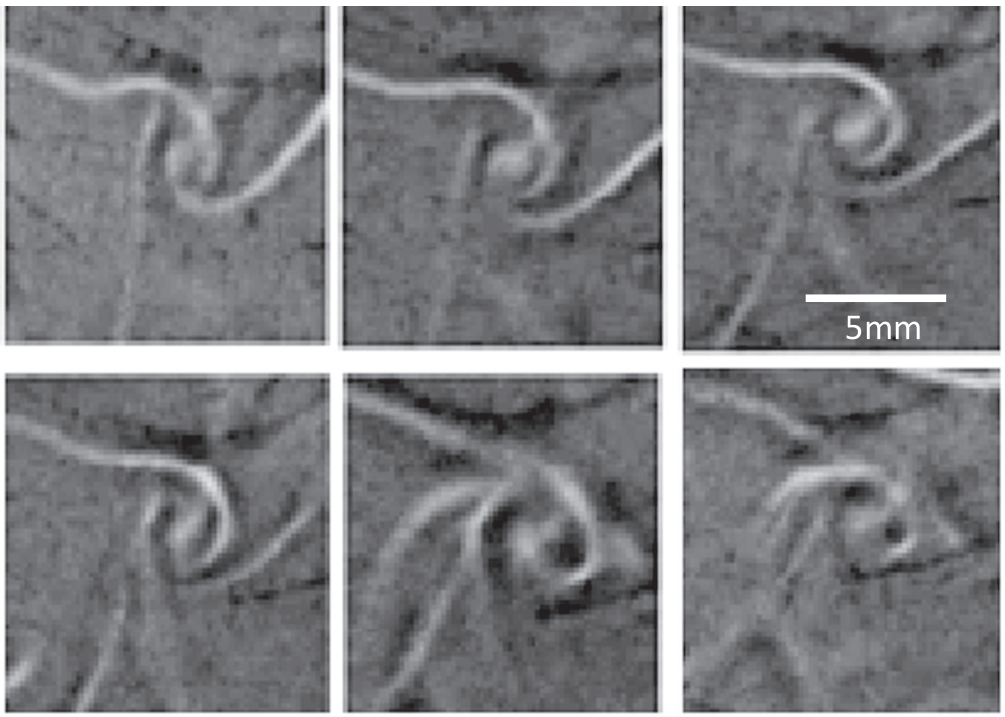

Figure 7. The sequence of images shows the time evolution for the interaction between focusing with opposite curvature generating vortex-like features. The time duration of the process was ∼1 s.

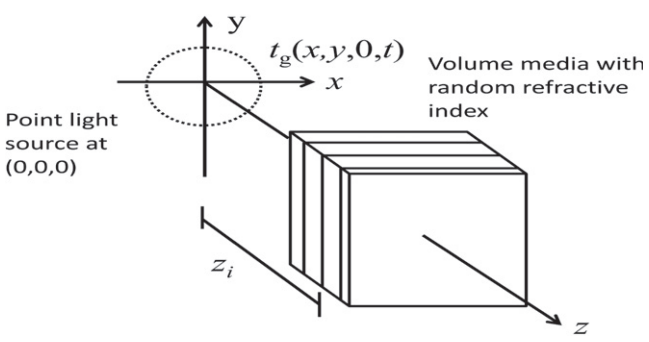

Figure A.1. The Fraunhofer diffraction field is generated on the source plane. It is easily identified by watching the source trough the random media.

Consequently, it is possible to associate a single one transmittance function t_g, whose representation corresponds with the inverse Fourier transform of the Fraunhofer diffraction field given by

$$t_g(x, y, t) = F^{-1} \times \left(T_1(u, v, t) \otimes T_2(u, v, t) \ldots \otimes T_n(u, v, t)\right). \quad \text{(A.4)}$$

Following this kind of analysis, it is possible to match the transmittance function $\boldsymbol{t_g}$ with a rough surface. It can be understood by considering the rough surface as a set of thin slices, justifying in this way the equivalence between the light propagation through the volume media with random refractive index and a rough surface.

Appendix B. Diffusion process for the focusing regions

In this section, we justified the diffusion process that may occur in the neighborhood of the focusing regions. The parameters involved in the analysis are sketched in figure 2. For the analysis, we define $f(s,t)$ as a function associated to the density of rays in the neighborhood of the focusing region. It is related to the irradiance function by

$$I(s, t) = af(s, t)\Delta A, \quad \text{(B.1)}$$

where ΔA is the element of area perpendicular to the focusing region and a is a constant of proportionality. Taking the time partial derivative of the irradiance function, we have

$$a\Delta A\frac{\partial f(s, t)}{\partial t} = \frac{\partial I}{\partial t}. \quad \text{(B.2)}$$

Taking now the derivative of the density of rays, when the arc length increases a distance Δs, we obtain

$$a\Delta s\Delta A\frac{\partial f(s, t)}{\partial s} = \Delta s\frac{\partial I}{\partial s} = \Delta t\frac{\partial I}{\partial t}, \quad \text{(B.3)}$$

where Δt is the time that takes the focusing region in increase

a distance Δs. We can re-write the last equation as

$$\frac{\Delta s}{\Delta t}\frac{\partial I(s,t)}{\partial s} = \frac{\partial I}{\partial t}. \tag{B.4}$$

The speed of changes of the focusing region is given by $v = \frac{\Delta s}{\Delta t}$, consequently, last expression acquires the form

$$v\frac{\partial I(s,t)}{\partial s} = \frac{\partial I}{\partial t} \tag{B.5}$$

The term $vI(s,t)$, describe the change of the irradiance function, which is redistributed along the arc of length, then we have

$$vI(s,t) = b\frac{\partial I(s,t)}{\partial s}, \tag{B.6}$$

which can be consider as the Fick's law, where b is another constant of proportionally. Substituting (B.6) in (B.5) we finally obtain

$$\frac{\partial^2 I(s,t)}{\partial^2 s} = D\frac{\partial I}{\partial t}, \tag{B.7}$$

which is the diffusion equation and D is the diffusion constant.

References

[1] Struik D J 1998 *Lectures on Classical Differential Geometry* (New York: Dover)
[2] Graustein W C 2006 *Differential Geometry* (New York: Dover) pp 79–103
[3] Kivshar Y S and Ostrovskaya E A 2001 *Opt. Photonics News* **12** 24–8
[4] Rhodes D P, Lancaster G P T, Lancaster J, Mcgloin D, Arlt J and Dholakia K 2002 *Opt. Commun.* **214** 247–54
[5] Martinez-Niconoff G, Carranza J and Rodriguez A C 1995 *Opt. Commun.* **114** 194–8
[6] Berry M V and Upstill C 1980 Catastrophe optics: morphologies of caustics and their diffraction patterns *Progress in Optics* vol 8 ed E Wolf (New York: Elsevier)
[7] Kivshar Y S and Pelinovsky D E 2000 *Phys. Rep.* **331** 117–95
[8] Martínez niconoff G, Mendez E, Martínez Vara P and Carbajal Dominguez A 2004 *Opt. Commun.* **239** 259–63
[9] Martínez-Niconoff G, Munoz-Lopez J, Silva-Barranco J, Carbajal-Domínguez A and Martínez-Vara P 2012 *Opt. Lett.* **37** 2121–3
[10] Basistiy I V, Bazhenov V Y, Soskin M S and Vasnetsov M V 1993 *Opt. Comm.* **103** 422–8
[11] Teague M R 1982 *J. Opt. Soc. Am.* **72** 1199–209
[12] Streibl N 1984 *Opt Commun.* **49** 6–10
[13] Hoel H, Port S C and Stone C J 1972 *Introduction to Stochastic Processes* (Boston: Houghton Mifflin Co.)
[14] Wasserman L 2004 *All of Statistics* (Berlin: Springer)
[15] Nye J F 1999 *Natural Focusing and Fine Structure of Light* (Bristol: IOP Publishing)